Production of nanocellulose using controlled acid hydrolysis from large-scale production of micro-fibrillated cellulose derived from oil palm empty fruit bunches

Production of nanocellulose using controlled acid hydrolysis from large-scale production of micro-fibrillated cellulose derived from oil palm empty fruit bunches

F Yurid[1], A S Handayani[2], F D Maturbongs[3], Y Irawan[4], Y Sampora[4], Y A Devy[4], M Septiyanti[4], D Ramdani[4], E Supriadi[4], K N M Amin[5], and A A Septevani[1,2*]

[1] Research Center for Environmental and Clean Technology, National Research and Innovation Agency, KST BRIN Cisitu, Bandung 40135, Indonesia
[2] Department of Chemical Engineering, Institut Teknologi Indonesia, Jl. Raya Puspiptek Serpong, South Tangerang 15314, Indonesia
[3] PT Mandiri Palmera Agrindo, Jakarta 12930, Indonesia
[4] Research Center for Chemistry, National Research and Innovation Agency, KST BRIN Serpong, South Tangerang 15314, Indonesia
[5] Faculty of Chemical and Process Engineering Technology, Universiti Malaysia Pahang, Leburaya Tun Razak, Pahang D.M 26300, Malaysia
*E-mail: athanasia.amanda.septevani@brin.go.id

Abstract. Nanocellulose is generally known as a versatile material, which is suitable for various applications due to its unique physicochemical properties, including light weight, ease of tunable surface functionalization, and excellent mechanical properties. This research aims to characterize and synthesize nanocellulose produced from acid hydrolysis of large-scaled micro-fibrillated cellulose (MFC) derived from oil palm empty fruit bunches by varying concentrations of H_2SO_4 from 20 to 35 v/v %. The obtained large-scaled MFC had a density of 1.01 kg/m^3 and was dominantly composed of 71% cellulose. After acid hydrolysis of MFC, there were gradual changes in the colour of the obtained cellulose nanocrystals (CNC) dispersion from light white to a darker color with the increase of acid concentration, in which the over hydrolysis occurs at 35% of acid concentration. The use of 25-30% H_2SO_4 showed the optimum condition to avoid over-hydrolysis and resulted in bright white color of CNC dispersion with excellent stability at zeta potential value of -74.2±0.1 to -88.4±0.2 mV. It was supported by Fourier transform infrared (FTIR) due to the presence of negatively charged sulfonyl and hydroxyl groups upon CNC formation to offer excellent dispersion stability. Based on transmission electron microscope (TEM), rod-like shape CNC with a low aspect ratio of 11.8 at the dimension of 12.8 ± 6.7 nm in width and 151.9 ± 38.3 nm in length was successfully produced. Based on X-ray diffraction (XRD) analysis, the crystallinity of the sample was 76%.
Keywords: acid hydrolysis; micro-fibrillated cellulose; nanocellulose; oil palm empty fruit bunches

1. Introduction

Nanocellulose has attracted a greater interest to be developed as a new renewable nanomaterial due to its excellent mechanical strength and unique chemical properties [1]. It is also known that nanocellulose offers a high crystallinity and nicely fibrous morphology in various dimensions, low toxicity, and tuneable surface functionalities [2–4]. Recently, nanomaterials derived from biomass sources have been

preferred because they are highly capable of mass scale-production due to biological abundance in addition to renewable and sustainable sources with less environmental impact [5].

Nanocellulose can be obtained in various types of morphology, such as rod-like shape, filament/long, and sphere-like shape structures, depending on their preparation types. Among them, rod-like shape cellulose nanocrystals (CNC) are considered the most commonly used nanocellulose in various applications due to high crystalline forms with a length typically less than 500 nm leading to a low aspect ratio and more increased transparency [6,7]. Nanocellulose from many biomass sources can be synthesized in many ways, such as enzymatic or acid hydrolysis, ionic liquid treatment, oxidation process, and mechanical method [8]. Among these methods, acid hydrolysis is the most effective process of producing CNC using organic or mineral acids, i.e., sulphuric acid, phosphoric acid, hydrobromic acid, or hydrochloric acid [9–12]. Sulphuric acid (H_2SO_4) has been the most extensively used in CNC production due to higher dispersion stability with the excellent surface of charges of the obtained CNC. Alongside an excellent stabilization of dispersion, some other advantages include higher crystallinity and more uniform size with a narrow poly-dispersity production of CNC.

Nanocellulose can be prepared from various resources of plant and non-plant (bacteria, tunicate, and algae) raw materials [13–15]. Non-wood resources, particularly from solid residues or wastes, are one of the promising materials to be developed into nanocellulose, which can benefit the reduction of environmental pollution while giving added value to the abundantly available waste. From oil plant plantations, the largest solid waste is oil palm empty fruit bunches (OPEFB) beside fronds and trunks. It can reach 30-35% of waste from fresh fruit bunches per harvest. OPEFB is known to comprise a high cellulose content (about 40-43%) [16]. Therefore it has the potential to be investigated for CNC production. Depending on the types of resources, methods, and even geographical location of the plant, the process and optimum condition of the production of CNC can vary due to the unique structures of each biological and genetic plant's cell wall properties.

In our previous study, we successfully extracted micro-fibrillated cellulose (MFC) from OPEFB using the large-scale pilot plant [17]. In the current study, production of nanocellulose was prepared from the large-scaled OPEFB MFC through the acid hydrolysis method by varying concentrations of H_2SO_4 at the range of 20-35% according to our previous findings [7,17] that are required to be further investigated depending on current typical obtained MFC. The properties of obtained nanocellulose were analyzed and compared to MFC in terms of chemical structure, morphology, and crystallinity.

2. Materials and methods

2.1. Materials

OPEFB was supplied from the oil palm plantations of PT. Mandiri Palmera Agrindo, in Luwu, Sulawesi Tengah, Indonesia. Other materials for the preparation of MFC, including the technical grade of sodium hydroxide (NaOH) and hydrogen peroxide (H_2O_2), as well as pH paper (Merck), were used as received. The technical grade sulphuric acid (H_2SO_4) 98% was purchased and used as received for acid hydrolysis.

2.2. Methods

2.2.1. Pre-treatment process. The pre-treatment process of OPEFB is the essential stage before acid hydrolysis to isolate cellulose from lignin and hemicellulose in OPEFB. This stage was adapted from our previous studies [18], consisting of several processes, including chopping and grinding to produce fine-size dried fiber of OPEFB, followed by simultaneous alkaline and bleaching processes using hydrogen peroxide (H_2O_2). This simultaneous process was conducted in a large-scale pilot plant facility in the Research Center for Chemistry-BRIN with a 50 kg raw OPEFB/ batch process capacity.

2.2.2. Isolation of nanocellulose (NCs) from OPEFB. The preparation of CNCs was adopted from our previous studies [17] by acid hydrolysis. The concentrations of H_2SO_4 were 20; 25; 30; and 35 v/v % at a temperature of 50 ºC for 3.5 hours and were denoted as CNC20; CNC25; CNC30; and CNC35, respectively. Subsequently, centrifugation was applied at 10,000 rpm for 10 minutes, followed by dialysis for 4-5 days to neutralize the obtained nanocellulose.

2.2.3. Characterization. The component analysis was done at the Integrated Testing Laboratory, Center for Standardization and Instrument for Sustainable Forest Management, Ministry of Environment and Forestry, Republic of Indonesia, Bogor, using the protocol of *Standar Nasional Indonesia* (SNI) 01-1303-1989. The study of stability of the CNC dispersion was carried out by observing from day 1 to day 30, then qualitatively proved by the zeta potential analysis within the ratio of sample to distilled water of 1:10 using Horiba Nano Partica SZ-100 at Research Center for Chemistry-BRIN. The morphological structure of nanocellulose from OPEFB was analyzed using TEM at the Faculty of Chemical and Process Engineering Technology, Universiti Malaysia Pahang. The CNC dispersion was spotted onto a carbon-coated formvar grid and stained with 1% aqueous uranyl acetate. The prepared samples were analyzed on a JEOL JEM 2100F Field Emission at 200 kV. The nanoparticle's aspect ratio (length/width) was determined based on TEM images using ImageJ software analysis. X-Ray analysis was conducted on a Shimadzu Maxima X-ray diffractometer (XRD-7000, Japan) generated at 40 kV and 30 mA at the Research Center for Advanced Material-BRIN. CNC samples were nicely placed in the sample holder and scanned over a range of 2θ from 10° to 35° with a speed of 2 min^{-1}. Then the crystallinity index (CrI) was calculated using Segal's method [7]. The functional groups were characterized using FTIR Bruker-Tensor II in a wavenumber range of 4000-500 cm^{-1} at The Research Center for Chemistry-BRIN.

3. Results and discussion

The pre-treatment process of OPEFB via alkaline treatment and bleaching process prior to the acid hydrolysis process is conducted to obtain high purity of cellulose. The combination of both bleaching and alkaline treatment ensures the removal of extractives, hemicelluloses, and lignin, to produce high-purity fibrillated cellulose, known as micro-fibrillated cellulose (MFC) [19]. Based on the component analysis, the large-scale MFC in this study contained high cellulose of 71.99–78.15%, with 7.85–13.77% of hemicellulose and 3.97–11.25% of lignin. The obtained MFC was then further processed into nanocellulose.

3.1. The stability test of CNC and zeta potential value

The stability test of CNC dispersion was observed in a month. Microcellulose and nanocellulose are differed based on their dispersibility in water. Figure 1 shows obtained CNC from acid hydrolysis at several variations of H_2SO_4 concentration. Images from left to right represent the use of 20%; 25%; 30%; and 35% H_2SO_4, respectively.

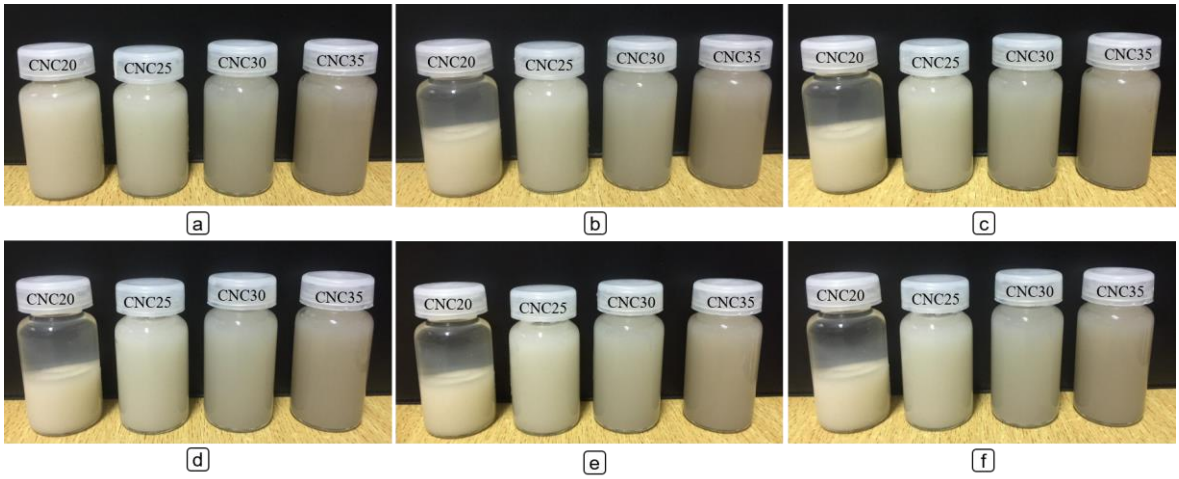

Figure 1. The photo of the observed stability test of CNC dispersion of a. Day 0; b. Day 1; c. Day 3; d. Week 1; e. Week 3; f. Week 4

As shown in Figure. 1, there was an increase in the stability of the CNC dispersion with increasing H_2SO_4 concentration. On the first day of observation, the dispersion of CNC20 was settled down (Figure

1b), while at higher acid concentrations than 25%, CNC dispersion was stable for up to a month. At the surface of nanocellulose, there is a more significant presence of negatively charged groups (hydroxyl and sulfonyl groups) compared to the microcellulose, creating a greater repulsive charged interaction leading to better dispersion stability [7]. The presence of negatively surface-charged groups was supported by the zeta potential, as discussed below.

Figure 1 also shows the change in color of the resulting CNC, where the color was darker, along with the increasing H_2SO_4 concentration. The results showed that CNC35 at 35% H_2SO_4 concentration showed the darkest color among other CNC dispersions, indicating an over-hydrolysis [18]. To understand and confirm the behavior of CNC upon acid hydrolysis at varied acid concentrations, surface charge analysis of CNC was conducted by using zeta potential analyzer, which is shown in Table 1,

Table 1. Zeta potential value of CNCs

Samples	Mean (mV)		
CNC20	-19.4	±	0.2
CNC25	-74.2	±	0.1
CNC30	-88.4	±	0.2
CNC35	-45.5	±	0.4

Table 1 shows the increase of negative charge of zeta potential along with the increasing H_2SO_4 concentration up 30%, but then it decreased significantly at the concentration of 35%. It is reported that zeta potential above -30 mV indicates the successful formation of typical nano-scale material dispersion [20] as expected on CNC25 to CNC35. Below -30 mV, the agglomeration and weaker dispersion stability, as normally observed in the micro-scale structure, were obtained. The result agreed with the formation of two-phase separation of CNC20 (Figure 1b) with a zeta potential value at only -19.4 mV. The increasing sulphuric acid concentration increased the zeta potential, increasing the negative surface charge of hydroxyl and sulfonyl groups on the surface of CNC at a concentration ≥ 20%. However, the excess amount of H_2SO_4 concentration at 35% of H_2SO_4 had probably caused the over-hydrolysis of CNC, where the further deconstruction of the sugar chain in the cellulose structure occurred, leading to carbon formation [18]. It is responsible for the darker color of the CNC dispersion and eventually affected the decrease in zeta potential (-45.5±0.4 mV). Among the samples, CNC25 had a brighter white color with excellent zeta potential and was selected for further evaluation.

3.2. The functional group of CNC and MFC

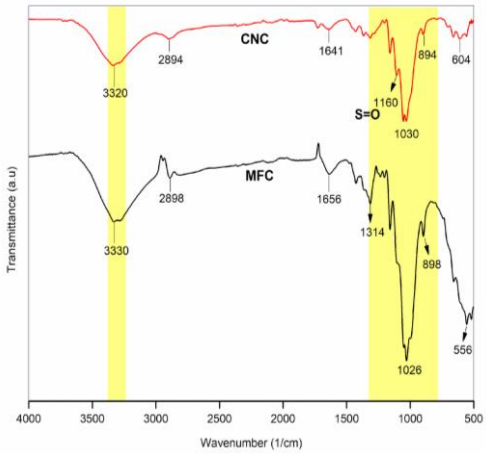

Figure 2. FTIR spectra of MFC and CNC25

All the spectra showed the characteristic peaks of cellulose. The asymmetric vibration bands around 2894-2898 cm^{-1} corresponded to C–H bonds [21,22]. Further, the peaks around 1030 and 1026 cm^{-1}

corresponded to C–O bonds, as well as the O–H bonds at spectra between 3600 and 3200 cm^{-1} were also observed for both CNC and MFC. The absorption peaks in the region of 894-898 cm^{-1} corresponded to the anomeric carbon group of the typical carbohydrate groups [23,24].

MFC showed distinctive aliphatic saturated C-H stretching at around 2898–2904 cm^{-1} attributed to the presence of methylene groups in the typical linear polymer structure of lignocellulose (lignin, cellulose, and hemicellulose) [25,26]. In addition, the spectra in the region of 1342–1305 cm^{-1} were observed, indicating the CH_2 rocking of polysaccharides [27,28]. The differences in CNC and MFC spectra can be seen based on the OH peak shifted from 3330 cm^{-1} for MFC to 3320 cm^{-1} for CNC. It has been known that the amorphous structure, mostly found in MFC, possesses high flexibility and, thus, high signaling stretching intensity on the OH region at 3330-3320 cm-1. In contrast, the lower intensity peak was observed at 3320 cm^{-1} in the CNC spectrum, indicating the higher crystallinity of CNC [29,30], and was confirmed in XRD, as discussed in the following subsection.

Furtherly, the shifting spectra from 2898 cm^{-1} for MFC into 2894 cm^{-1} for CNC and 898 cm^{-1} for MFC to 894 cm^{-1} for CNC was also observed. All the results represent that the cleavage of a glycosidic bond and a long cellulose chain was broken upon hydrolysis from the amorphous MFC structure into crystallite nanocellulose. Further, the peaks at 1160 cm^{-1} and 604 cm^{-1} associated with the presence of sulfonate group (SO_2) and SO_2 scissoring, as typically observed on the active surface group on CNC upon sulphuric acid hydrolysis, were evidently observed in FTIR spectra of the obtained CNC in this study [18,27,31,32].

3.3. The crystallinity of CNC and MFC

Before hydrolysis, the cellulose content in the MFC samples is composed of both crystalline and amorphous regions. The disordered (amorphous) region is attacked by the presence of acid. While at the same time, the highly ordered crystalline remains stable upon acid hydrolysis, thus increasing the crystallinity index of the obtained CNC. The degree of crystallinity was investigated on the selected CNC and compared to MFC (Figure 3) using XRD. All the samples showed three reflections characteristic for cellulose at 2θ= 16°, 23° and 34.5°, which correspond to the (1 1 0), (2 0 0), and (0 0 4) crystallographic planes of cellulose [33,34]. The major and single crystalline peak was observed at 23° in the CNC spectra, confirming the presence of crystalline cellulose [35]. These results show that crystal structures of the cellulosic substrates remained unchanged and stable during acid hydrolysis.

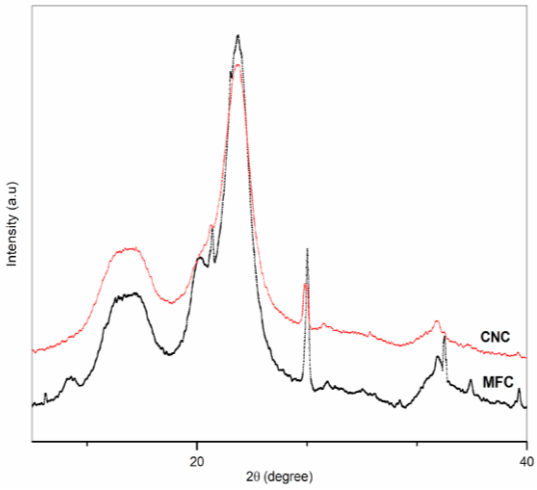

Figure 3. X-ray diffraction spectra of CNC25 and MFC

Further, the crystallinity percentages were calculated with Segal's method, where the value for the obtained CNC and MFC in this study was 76% and 67%, respectively. The crystallinity index of obtained CNC was in agreement with other studies with similar resources from OPEFB at 73–77.1% [7,36]. Besides, the MFC sample was compared to other biomass resources, such as sugarcane bagasse-

MFC, which has a lower crystallinity than the obtained OPEFB-MFC at a maximum crystallinity of 47% [33]. Moreover, the crystallinity of the obtained CNC from strong acid hydrolysis also showed a higher crystallinity compared to OPEFB-CNC produced from mechanical via high-pressure homogenizer at the maximum crystallinity of 69% [37].

3.4 The Morphology of CNC

The morphology of obtained CNC was investigated using TEM. Figure 4 shows the TEM images of the selected CNC. As can be seen from Figure 4, a rod-like shaped nanocellulose from OPEFB was successfully produced via strong acid hydrolysis.

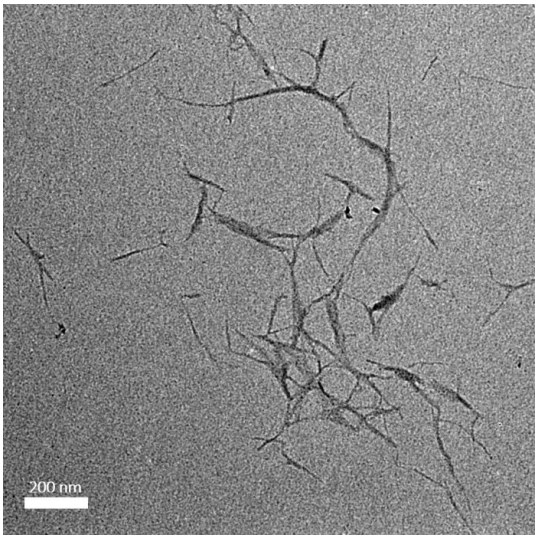

Figure 4. TEM image of CNC25

Based on the ImageJ software, CNC had a low aspect ratio of 11.8 at the dimension of 12.8 ± 6.7 nm in width and 151.9 ± 38.3 nm in length. Moreover, the size of CNC is uniform with a needle-like structure which is in agreement with other CNC structures derived from other resources such as cotton [4]. Figure 4 shows that the individual nanocellulose has been uniformly dispersed in the matrix, and no agglomeration of nanocellulose was observed. The sulfate groups (SO_4^{2-}) in the CNC give a negative surface charge, which enables the CNC to be dispersible in water [6], as also noted by high surface charge intensity up to -74 mV observed in Table 1. Similar results have also been reported in a previous study by Prataphan et al. (2016) [38], which produced a rod-like nanocellulose from microcrystalline cellulose (MCC) via strong acid hydrolysis method offering higher surface charge intensity and thus excellent dispersibility in water.

4. Conclusion

In this study, alkaline treatment and bleaching processes were used to isolate cellulose from oil palm empty fruit bunches (OPEFB) using a large-scale facility at BRIN. The isolated cellulose was then hydrolyzed by varying concentrations of H_2SO_4 (20; 25; 30; 35) v/v% to produce CNC. At 25-30%, H_2SO_4 showed the optimum condition to avoid over-hydrolysis and resulted in bright white color of CNC dispersion with excellent stability at a potential value of -74.2±0.1 to -88.4±0.2 mV. Based on TEM and XRD, rod-like shape CNC with a low aspect ratio of 11.8 at the dimension of 12.8 ± 6.7 nm in width and 151.9 ± 38.3 nm in length with a crystallinity of 76% were successfully produced.

Acknowledgment

Authors are grateful to acknowledge financial support from PT Mandiri Palmera Agrindo for the large-scale production of MFC and Prioritas Nasional Energi Baru Terbarukan OREM-BRIN for the production of nanocellulose via acid hydrolysis. The TEM analysis was supported by Kedaireka

Matching Funds 2022 – Institut Teknologi Indonesia and assisted by the Faculty of Chemical and Process Engineering Technology, Universiti Malaysia Pahang. The authors are also grateful for the analysis support from E-Layanan Sains (ELSA), the National Research and Innovation Agency (BRIN).

Author contributions

A A Septevani contributed to the study conception and experimental design. F Yurid and A.A. Septevani conducted data analysis and manuscript writing. A S Handayani, F D Martubongs, Y Irawan, Ramdani, and E Supriadi carried out the MFC production. F Yurid, A.A. Septevani, Y Sampora, and Y A Devy conducted the preparation of nanocellulose from the obtained MFC. M Septiyanti assisted with the analysis of zeta potential and interpretation, while K N M Amin assisted with the TEM analysis and interpretation. All authors read and approved the final manuscript.

References

[1] Aulin C, Karabulut E, Tran A, Waìšgberg L and Lindström T 2013 *ACS Appl. Mater. Interfaces* **5** 7352–9
[2] Eichhorn S J 2011 *Soft Matter* **7** 303–15
[3] Bian H, Chen L, Dai H and Zhu J Y 2017 *Cellulose* **24** 4205–16
[4] Septevani A A, Evans D A C, Annamalai P K and Martin D J 2017 *Ind Crops Prod* **107** 114–21
[5] Seta F T, An X, Liu L, Zhang H, Yang J, Zhang W, Nie S, Yao S, Cao H, Xu Q, Bu Y and Liu H 2020 *Carbohydr. Polym.* **234** 115942
[6] Moon R J, Martini A, Nairn J, Simonsen J and Youngblood J 2011 *Chem. Soc. Rev.* **40** 3941-94
[7] Septevani A A, Burhani D, Sampora Y, Indriyati, Shobih, Rosa E S, Sondari D, Margyaningsih N I, Septiyani M, Yurid F and Handayani A S 2022 *J. Polym. Environ.* **30** 3901–13
[8] Mohd Amin K N, Annamalai P K, Morrow I C and Martin D 2015 *RSC Adv.* **5** 57133–40
[9] Viet D, Beck-Candanedo S and Gray D G 2007 *Cellulose* **14** 109–13
[10] Frost B A and Johan Foster E 2020 *J. Renew. Mater.* **8** 187–203
[11] Yu H, Qin Z, Liang B, Liu N, Zhou Z and Chen L 2013 *J Mater Chem A* **1** 3938–44
[12] Chen L, Zhu J Y, Baez C, Kitin P and Elder T 2016 *Green Chem.* **18** 3835–43
[13] Septevani A A, Evans D A C, Hosseinmardi A, Martin D J, Simonsen J, Conley J F and Annamalai P K 2018 *Small* **14** 1–6
[14] Burhani D, Septevani A A, Setiawan R, Djannah L M, Putra M A, Kusumah S S and Sondari D 2021 *Polymers* **13** 1–14
[15] Lubis R, Wirjosentono B, Eddyanto and Septevani A A 2020 *Colloids Surf. A Physicochem. Eng. Asp.* **604** 125311
[16] Zhou Y M, Fu S Y, Zheng L M and Zhan H Y 2012 *Express Polym. Lett.* **6** 794–804
[17] Septevani A A, Burhani D, Sampora Y, Devy Y A, Ariani G N, Sudirman S, Sondari D and Mohd Amin K N 2019 *Jurnal Kimia Terapan Indonesia* **21** 31–7
[18] Septevani A A, Rifathin A, Sari A A, Sampora Y, Ariani G N, Sudiyarmanto and Sondari D 2020 *Carbohydr. Polym.* **229** 115433
[19] Trilokesh C and Uppuluri K B 2019 *Sci. Rep.* **9** 1–8
[20] Yang X, Han F, Xu C, Jiang S, Huang L, Liu L and Xia Z 2017 *Ind Crops Prod* **109** 241–7
[21] Xu F, Yu J, Tesso T, Dowell F and Wang D 2013 *Appl. Energy* **104** 801–9
[22] Robles E, Fernández-Rodríguez J, Barbosa A M, Gordobil O, Carreño N L V and Labidi J 2018 *Carbohydr. Polym.* **183** 294–302
[23] Lu P and Hsieh Y Lo 2010 *Carbohydr. Polym.* **82** 329–36
[24] Gallardo-Sánchez M A, Diaz-Vidal T, Navarro-Hermosillo A B, Figueroa-Ochoa E B, Casillas R R, Hernández J A, Rosales-Rivera L C, Martínez J F A S, Enríquez S G and Macías-Balleza E R 2021 *Nanomaterials* **11** 1–21
[25] Fahma F, Iwamoto S, Hori N, Iwata T and Takemura A 2010 *Cellulose* **17** 977–85
[26] Liu C, Li B, Du H, Lv D, Zhang Y, Yu G, Mu X and Peng H 2016 *Carbohydr. Polym.* **151** 716–24

[27] Chieng B W, Lee S H, Ibrahim N A, Then Y Y and Loo Y Y 2017 *Polymers* **9** 1–11
[28] Phanthong P, Guan G, Ma Y, Hao X and Abudula A 2016 *J Taiwan Inst Chem Eng* **60** 617–22
[29] O'connor R T, Dupré E F and Mitcham D 1958 *Text. Res. J.* **28** 382–92
[30] Lu P and Hsieh Y Lo 2012 *Carbohydr. Polym.* **87** 564–73
[31] Souza N F, Pinheiro J A, Brígida A I S, Morais J P S, de Souza Filho M de sá M and de Freitas Rosa M 2016 *Ind Crops Prod* **94** 480–9
[32] Cheng M, Qin Z, Chen Y, Hu S, Ren Z and Zhu M 2017 *ACS Sustain. Chem. Eng.* **5** 4656–64
[33] Grande R, Trovatti E, Pimenta M T B and Carvalho A J F 2018 *J Renew Mater* **6** 195–202
[34] Sun X, Wu Q, Ren S and Lei T 2015 *Cellulose* **22** 1123–33
[35] Rosa M F, Medeiros E S, Malmonge J A, Gregorski K S, Wood D F, Mattoso L H C, Glenn G, Orts W J and Imam S H 2010 *Carbohydr. Polym.* **81** 83–92
[36] Ngadi, N. Lani, N.S. , Johari, A. , Jusoh M 2014 *J. Nanomater.* **2014**
[37] Jonoobi M, Khazaeian A, Tahir P M, Azry S S and Oksman K 2011 *Cellulose* **18** 1085–95
[38] Prathapan R, Thapa R, Garnier G and Tabor R F 2016 *Colloids Surf. A Physicochem. Eng. Asp.* **509** 11–8